Journal of Applied Polymer Science

Fabrication and Characterization of Novel Hyperbranched Polyimides with Excellent Organosolubility, Thermal and Mechanical Properties

Wenqiu Chen,[1,2] Quantao Li,[2] Quanyuan Zhang,[1,2] Zushun Xu,[1,2] Xianbao Wang,[1,2] Changfeng Yi[1,2]

[1]Hubei Collaborative Innovation Center for Advanced Organic Chemical Materials, Wuhan 430062, People's Republic of China

[2]Ministry of Education Key Laboratory for the Green Preparation and Application of Functional Materials, Hubei University, Wuhan 430062, People's Republic of China

Correspondence to: C. Yi (E-mail: changfengyi@hubu.edu.cn)

ABSTRACT: A series of amine-terminated and anhydride-terminated hyperbranched polyimides (HBPIs) were successfully prepared with various commercial dianhydrides and a novel BB'_2-type aromatic triamine, 2,4,6-tris[4-(4-aminophenoxy)phenyl]pyridine, with a symmetrical triaryl-substituted pyridine segment and prolonged flexible linkages. The chemical structure of the triamine monomer and the hyperbranched structure of the resulting polymers were verified by Fourier transform infrared spectroscopy and ^{1}H-NMR spectroscopy. The resulting HBPIs, which mainly held an amorphous morphology, exhibited improved organosolubilities in several strong polar aprotic solvents, good heat resistance with glass-transition temperature values in the range 218.6–311.0°C, and excellent thermal stabilities in both N_2 and air [the temperature at 5% weight loss ($T_{5\%}$) in N_2 was higher than 529.8°C and the $T_{5\%}$ in air was higher than 465.1°C]. The obtained HBPI films also showed outstanding mechanical properties with tensile strength, tensile modulus, and elongation at break values of 86.4–101.3 MPa, 1.73–2.04 GPa, and 5.07–10.67%, respectively; considerable optical transparency; low water absorption; and neutral interface wettability. © 2014 Wiley Periodicals, Inc. J. Appl. Polym. Sci. **2015**, *132*, 41544.

KEYWORDS: hyperbranched polymers; mechanical properties; polyimide; thermal properties

Received 24 July 2014; accepted 19 September 2014

DOI: 10.1002/app.41544

INTRODUCTION

Aromatic polyimides (PIs) are one of the most significant and promising classes of high-performance polymers with their high strength and modulus values, incomparable high-temperature stability, and excellent chemical resistance. They are widely used as coatings, adhesives, membranes, foams, fibers, and matrix materials and are applied numerously in the microelectronics, semiconductor, aerospace, and optoelectronics industries.[1–4] However, further research and applications of wholly aromatic PIs are often confined because of their numbered solubility in most organic solvents and the poor processability, which is due to their high softening temperatures or melting temperatures. Therefore, most of the recent research focus is on the fabrication of processable PIs and the incorporation of new functionalities to make the polymers more tractable without a deterioration of their own outstanding comprehensive properties.[5–7] Various efforts have focused on the design and synthesis of novel amine or anhydride monomers with bulky substituents[8,9] or twisted[10] or unsymmetrical[11] structures to impart polymers with good organosolubilities or melt-processing characteristics. In addition, the introduction of flexible linkages, for instance, —O—, —S—, —CO—, —SO_2—, —$C(CH_3)_2$—, and —$C(CF_3)_2$—,[12–16] into the polymer backbones will increase the disorder and winding of the polymer chains; this will result in a decrease in chain-to-chain interactions and the chain-packing efficiency to hinder the crystallization of polymers. Consequently, the organosolubility and heat processability will significantly improve compared with polymers without these linkages.

Pyridine and its derivatives have been proven to possess excellent high-temperature stability, chemical stability, and favorable polarity and dielectric properties because of its aromatic heterocyclic structure.[17,18] Furthermore, the pyridine ring, with a localized lone pair of electrons in the sp^2 orbital, can be easily protonized by acids or coordinated with various metal ions; this augments the solubility of the heterocycle or heterochain polymers containing pyridine moieties in the backbone and offers the possibility of further functional modifications.[19] Recently, Liaw and coworkers,[20–22] Wang and coworkers,[23–25] Shang et al.,[26] and our team[27–31] have successively introduced the symmetrical triaryl-substituted pyridine structure into PI backbones. The resulting PIs have been found to exhibit excellent thermal stabilities, good organosolubilities, and considerable mechanical

properties. Some have even showed favorable photoelectronic properties. Nonetheless, according to our knowledge of the literature, almost all studies of PIs with symmetrical triaryl-substituted pyridine backbones or/and flexible linkages that have been reported are linear polymers.

Ever since they were first reported by Flory in 1952,[32] hyperbranched polymers have attracted increasing attention because of their unique structural characteristics, excellent physical and chemical properties, and especially, a large number of terminal groups, which could be functionalized compared to their linear analogues. In the latest 2 decades, some investigators have successively prepared various HBPIs, which not only inherited the excellent properties of PIs, such as high-temperature stabilities and high strength, but also presented good organosolubilities, a low solution viscosity, and noncrystalline properties, which resulted from their hyperbranched structure.[33–37] However, most of the studies on HBPIs have focused only on the structural characterization, basic physical properties, and potential applications, seldom have involved research on further applications with other superior properties. Moreover, the aforementioned HBPIs, which were obtained in the presence of larger quantities of solvents than the linear ones, were unavailable to prepare strong and tough thin films with excellent mechanical strength[38] because of the relatively low molecular weight and insignificant chain entanglements in the solid state.

In our previous works, PIs with symmetrical triaryl-substituted pyridine backbone and hyperbranched structure were found to present severely limited organosolubilities and mechanical strengths because of their strong rigidity of the backbones.[39] Moreover, HBPIs derived from a novel triamine monomer with a metasubstituted asymmetrical structure and prolonged chain segments were found to have not only inheriting excellent thermal properties but also considerable organosolubilities and good mechanical properties.[40] Herein, we did some extending and relatively parallel attempts in which a novel BB'_2-type aromatic triamine monomer, 2,4,6-tris[4-(4-aminophenoxy)phenyl]pyridine (TAPPP), was synthesized and further used to prepare a series of HBPIs with different terminal groups. We expected that the simultaneous introduction of an symmetrical triaryl-substituted pyridine segment and prolonged flexible diphenyl ether linkages would increase the flexibility of the branched chains and prolong the length between branching points; this resulted further in the augmentation of a number of chain entanglements. This would eventually allow us to improve the organosolubility, enhance the mechanical properties, and maintain the outstanding thermal properties. The general physical properties, optical transparency, and water resistance of the obtained HBPIs were also investigated. Further research on applications with other superior properties will be done in our subsequent works.

EXPERIMENTAL

Materials

4-Hydroxyacetophenone (99%), 4-hydroxybenzaldehyde (99%), 1-chloro-4-nitrobenzene (99%), palladium on activated carbon (Pd/C; 5%), hydrazine monohydrate (80 vol %), glacial acetic acid (AcOH), and ammonium acetate ($AcONH_4$) were purchased from Aladdin Reagent, Inc. (Shanghai, China), and were used as received. 3,3′,4,4′-Benzophenonetetracarboxylic dianhydride (BTDA) and 4,4′-(hexafluoroisopropylidene) diphthalic anhydride (6FDA) were obtained from J & K Scientific, Ltd. (Beijing, China). 4,4′-Oxydiphthalic dianhydride (ODPA) and 2,2-bis[4-(3,4-dicarboxyphenoxy) phenyl] propane dianhydride (BPADA) were purchased from Shanghai Research Institute of Synthetic Resins (Shanghai, China). These aromatic tetracarboxylic dianhydrides were all recrystallized from acetic anhydride and then dried *in vacuo* at 120°C for 12 h before use. *N*-Methyl-2-pyrrolidone (NMP) and *m*-xylene were distilled from calcium hydride under reduced pressure. Anhydrous potassium carbonate (K_2CO_3; analytical reagent) was dried *in vacuo* at 120°C for 12 h before use. All other chemicals were obtained from various commercial sources and used without further purification.

Measurements

The Fourier transform infrared (FTIR) spectra were recorded on a Nicolet iS50 spectrometer (Thermo Fisher Scientific). ^{1}H-NMR and ^{13}C-NMR spectra were performed on a Inova 600 residual spectrometer (Varian) at 600 MHz with tetramethylsilane as a reference and hexadeuterated dimethyl sulfoxide (DMSO-d_6) as a solvent. The inherent viscosity ($[\eta]$) was determined at a 0.8 g/dL concentration of HBPIs in NMP with an Ubbelohde capillary viscometer at 25 ± 0.2°C. The solubilities were measured in several different organic solvents by the dissolution of 10 mg of polymers in 5 mL of solvent at room temperature or an elevated temperature for 24 h. The weight-average molecular weight (M_w) and polydispersity index (PDI) were measured by PL-GPC 220 high-temperature chromatograph (Agilent Technology) with NMP containing 0.05*M* LiBr (1 mL/min) as the eluent at 100°C and polystyrene as a standard. X-ray diffraction (XRD) patterns were obtained on a D8-Advance diffractometer (Bruker, Germany) with a Cu Kα radiation source ($\lambda = 0.15418$ nm). Differential scanning calorimetry (DSC) was obtained on a DSC-7 differential scanning calorimeter (PerkinElmer) under an N_2 atmosphere through an increase in the temperature from 100 to 320°C at a rate of 5°C/min. The dynamic mechanical thermal analysis (DMTA) was performed with a Q800 DMA instrument (TA Instruments) at 1 Hz in the temperature range from 50°C to about 400°C at a heating rate of 5°C/min in air. Thermogravimetric analysis (TGA) was carried out with an SII Diamond thermogravimetric/differential thermal analyzer instrument (PerkinElmer) from room temperature to 800°C at a heating rate of 10°C/min under both air and N_2 atmospheres. The mechanical properties were measured on a CMT4104 electromechanical universal testing machine (Shenzhen SANS Testing Machine Co., Ltd., China) with 50×5 mm^2 films at a load of 100 N and a rate of 2 mm/min. Ultraviolet–visible (UV–vis) spectra were measured with a UV-3600 UV–vis spectrophotometer (Shimadzu, Japan) in the transmittance mode. The surface contact angle (SCA) tests were conducted on a JC2000 D instrument (Shanghai, China). Water absorption (WA) was measured by the immersion of completely dried HBPI films into deionized water at room temperature for 24 h, and we then wiped the water on the surface and weighed

the sample. The value was calculated with an equation from our previous work.[40]

Monomer Synthesis

2,4,6-Tris(4-hydroxyphenyl)Pyridine (THPP). A 500-mL, three-necked, round-bottomed flask fitted with a mechanical stirrer, a reflux condenser, and a nitrogen inlet was charged with a mixture of *p*-hydroxybenzaldehyde (12.21 g, 0.1 mol), *p*-hydroxyacetophenone (27.23 g, 0.2 mol), $AcONH_4$ (75 g), and glacial AcOH (100 mL). The mixture was heated under reflux with stirring for 3 h. Then, the mixture was poured into an excess of 50 vol % aqueous AcOH. The yellow precipitate was collected by filtration, recrystallized twice from ethanol/water, and dried at 80°C *in vacuo*.

Yield: 14.38 g (40.5 wt %). FTIR (KBr, cm^{-1}): 3295 (O—H); 1607, 1548, 1445 (C=N and C=C of pyridine). ^{1}H-NMR (600 MHz, DMSO-d_6, δ): 9.76 (s, 1H), 9.68 (S, 2H), 8.09–8.08 (d, 4H), 7.84 (s, 2H), 7.81–7.80 (d, 2H), 6.88–6.85(m, 6H).

2,4,6-Tris[4-(4-nitrophenoxy)-phenyl]Pyridine (TNPPP). To a completely dried 250-mL, four-necked, round-bottom flask equipped with a magnetic stirrer, a nitrogen inlet, a thermometer, and a Dean–Stark trap were added a mixture of compound THPP (14.38 g, 40.5 mmol), anhydrous K_2CO_3 (27 g), dimethylacetamide (DMAc; 180 mL), and toluene (72 mL). The mixture was stirred for 1 h and then refluxed (130°C) for another 3 h. After the mixture was cooled to 70°C, *p*-chloronitrobenzene (19.15 g, 121.5 mmol) was added. The mixture was then warmed to 130°C and kept at this temperature for 6 h. After most of the toluene was distilled, the experiment was conducted at 130°C for a further 24 h. After the solution was poured into an excess of ethanol and stirred overnight, the precipitate was collected by filtration, recrystallized from 2-methoxyethanol, and dried at 80°C *in vacuo* to give a dark yellow power.

Yield: 27.5 g (94.5 wt %). FTIR (KBr, cm^{-1}): 1587, 1342 (—NO_2); 1606, 1542, 1430 (C=N and C=C of pyridine). ^{1}H-NMR (600 MHz, DMSO-d_6, δ): 8.46–8.45 (d, 4H), 8.26–8.24 (m, 8H), 8.21–8.20 (d, 2H), 7.37–7.33 (m, 6H), 7.21–7.20 (m, 6H).

TAPPP. TNPPP (27.5 g), 5% Pd/C (1.1 g), absolute ethanol (300 mL), and dimethylformamide (DMF; 100 mL) were placed into a 250-mL, three-necked flask fitted with a magnetic stirrer, a condenser, and a dropping funnel. The reaction mixture was refluxed with stirring; this was followed by the dropwise addition of hydrazine monohydrate (80 mL) over a period of 1 h. After the addition was completed, the mixture was further refluxed for 24 h. The hot mixture was then filtered to remove Pd/C, and the filtrate was subsequently poured into an excess of deionized water. The resulting solid was collected, recrystallized from ethanol/water, and dried at 80°C *in vacuo* to give gray needle crystals.

Yield: 22.9 g (95.3 wt %). mp (by DSC): 204.6–205.0°C. FTIR (KBr, cm^{-1}): 3500–3300 (—NH_2); 1603, 1543, 1427 (C=N and C=C of pyridine). ^{1}H-NMR (600 MHz, DMSO-d_6, δ): 8.24–8.23 (d, 4H), 8.00 (s, 2H), 7.96–7.95 (d, 2H), 7.00–6.98 (m, 6H), 6.84–6.83 (m, 6H), 6.63–6.62 (m, 6H), 5.05 (s, 6H). Mass spectrometry (MS) mass-to-charge ratio (%): 628.25 (M^+). Anal. Calcd for $C_{41}H_{32}N_4O_3$ (628.72): C, 78.32%; H, 5.13%; N, 8.91%. Found: C, 78.30%; H, 5.15%; N, 8.89%.

Polymer Preparation

Amino-Terminated Hyperbranched Polyimides (AM-HBPIs). The general polymerization procedure is outlined in Scheme 2. A typical two-step procedure of AM-HBPI based on TAPPP and BTDA (AM-1) is as follows. TAPPP (0.629 g, 1 mmol) was dissolved in NMP (10 mL) in a 100-mL, thoroughly dried four-necked flask under N_2 flow. A solution of BTDA (0.322 g, 1 mmol) in NMP (15 mL) was then added dropwise through a dropping funnel for a duration of 1 h under magnetic stirring at 40°C. The mixture was further conducted for 12 h at 40°C to afford an amino-terminated hyperbranched poly(amic acid) solution. Then, *m*-xylene (20 mL) was added, and the mixture was heated to reflux for another 5 h with a Dean–Stark apparatus. After the mixture was cooled to room temperature, the solution was poured into ethanol. The precipitate was collected by filtration, washed with ethanol, and dried at 80°C *in vacuo*.

The other AM-HBPIs obtained from ODPA, BPADA, and 6FDA dianhydrides were referred as AM-2, AM-3, and AM-4, respectively.

Anhydride-Terminated Hyperbranched Polyimides (AD-HBPIs). An AD-HBPI based on TAPPP and BTDA (AD-1) was synthesized by the same procedure, except that a solution of TAPPP (0.315 g, 0.5 mmol) in NMP (10 mL) was added to the mixture of BTDA (0.322 g, 1 mmol) and NMP (15 mL) for a duration of 1 h. The anhydride-terminated hyperbranched poly(amic acid) solution was obtained after the mixture was conducted further for 12 h. Then, chemical imidization was carried out via the addition of acetic anhydride (3 g) and triethylamine (1 g) to the aforementioned mixture with stirring at 40°C for 24 h. The resulting solution was precipitated from ethanol, and the resulting precipitate was collected by filtration, washed with ethanol, and dried at 80°C *in vacuo*.

The other AD-HBPIs obtained from ODPA, BPADA, and 6FDA dianhydrides were referred as AD-2, AD-3, and AD-4, respectively.

HBPI Films Preparation

We obtained the HBPI films by casting the corresponding hyperbranched poly(amic acid) solutions, which were filtered through 1.0-μm syringe filters, on leveled clean glass plates. The casting procedure was conducted with thermal curing at 100°C for 12 h and 150, 200, 250, and 300°C each for 1 h in N_2.

RESULTS AND DISCUSSION

Monomer Synthesis

As shown in Scheme 1, the novel BB'_2-type aromatic triamine monomer TAPPP was obtained via a three-step synthetic route. First, THPP was synthesized via a modified Chichibabin reaction of 4-hydroxybenzaldehyde and 4-hydroxyacetophenone in the presence of $AcONH_4$. In this step, a symmetrical trihydroxyphenyl pyridine segment was introduced into THPP by the modified Chichibabin reaction; this was a facile way to prepare a substituted pyridine compound.[41,42] The FTIR spectrum of

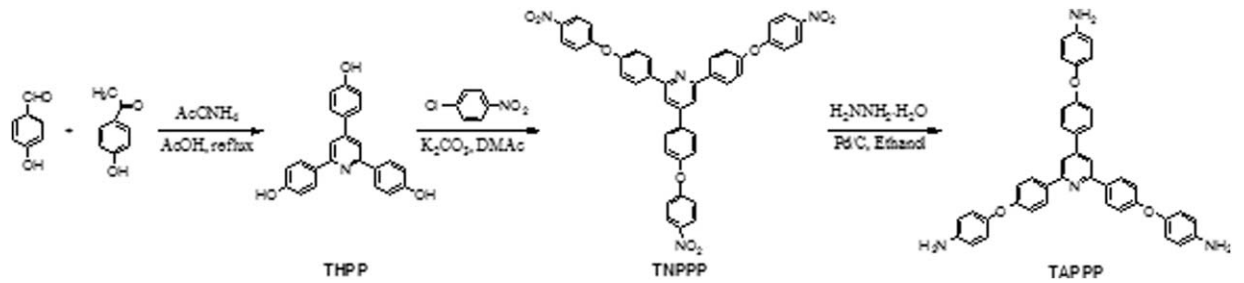

Scheme 1. Synthesis of the novel aromatic triamine monomer TAPPP.

THPP in Figure 1(a) showed a broad absorption band at 3380 cm^{-1} assigned to hydroxyl groups. In addition, the characteristic C═C and C═N bands of the phenyl and pyridine rings were also observed at 1430, 1550, and 1592 cm^{-1}. The ^{1}H-NMR spectrum of THPP in Figure 2(a) showed a single signal peak in turn at $\delta = 9.76$ (s, 1H) and $\delta = 9.68$ (s, 2H) due to the hydroxyl protons. In addition, the pyridine ring protons presented a single signal peak at $\delta = 7.84$ (s, 2H), and the other protons in the phenyl ring distributed in $\delta = 8.09$–8.09 (d, 4H), 7.81–7.80 (d, 2H), and 6.88–6.85 (d, 6H), respectively. Then, a trinitro compound TNPPP with a prolonged flexible diphenyl ether linkage was obtained by the nucleophilic substitution reaction of THPP and 4-chloronitrobenzene in the presence of anhydrous K_2CO_3. The characteristic absorptions of hydroxyl groups disappeared, and new absorptions at 1587 and 1342 cm^{-1}, which were attributed to nitro groups, appeared from the FTIR spectrum of TNPPP, as shown in Figure 1(b). The hydroxyl protons signal peaks also disappeared from the ^{1}H-NMR spectrum of TNPPP, as shown in Figure 2(b). Finally, the novel aromatic triamine TAPPP was obtained in a high yield by the reduction of TNPPP with hydrazine monohydrate catalyzed by Pd/C. The characteristic absorptions of nitro groups disappeared, and new absorptions at 3400 cm^{-1} attributed to amino groups appeared in the FTIR spectrum of TAPPP, as shown in Figure 1(c). The ^{1}H-NMR spectrum of TAPPP, as shown in Figure 2(c)m presented a new single signal peak at $\delta = 5.05$ (s, 6H), which could have been due to the amino protons. The other protons in the phenyl and pyridine ring are given in Figure 2(c). The ^{13}C-NMR spectrum of TAPPP was also obtained, and the assignments of the signal peaks are shown in Figure 2(d). The MS and elementary analysis results were in accordance with the theoretical values of TAPPP. The results indicate that the design and synthesis of the novel BB'_2-type aromatic triamine TAPPP was successful and feasible in this study. They also prove that TAPPP was pure enough with which to prepare HBPIs with various aromatic dianhydrides.

Polymer Preparation

As shown in Scheme 2, a series of AM-HBPIs and AD-HBPIs were prepared by the polymerization of the novel BB'_2-type aromatic triamine (TAPPP) with several commercially available A_2-type aromatic dianhydrides (BTDA, ODPA, BPADA, and 6FDA). The nonideal $A_2 + B_3$ polymerization, $A_2 + BB'_2$ polymerization with the resulting controllable polymer structure was used to prevent gelation.[33] The synthesis procedure was similar to the conventional two-step polymerization method for the

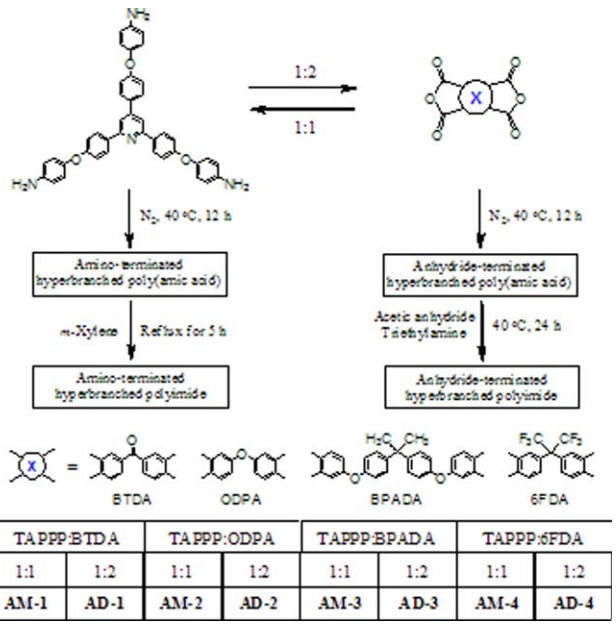

TAPPP:BTDA		TAPPP:ODPA		TAPPP:BPADA		TAPPP:6FDA	
1:1	1:2	1:1	1:2	1:1	1:2	1:1	1:2
AM-1	AD-1	AM-2	AD-2	AM-3	AD-3	AM-4	AD-4

Scheme 2. Synthesis of the novel HBPIs. [Color figure can be viewed in the online issue, which is available at wileyonlinelibrary.com.]

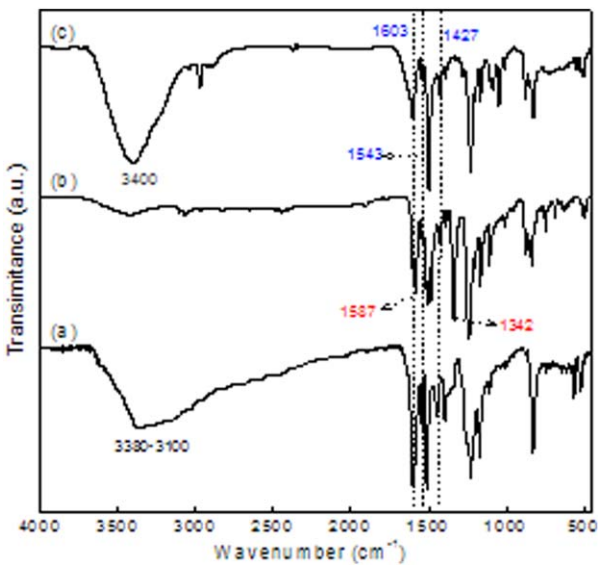

Figure 1. FTIR spectra of (a) THPP, (b) TNPPP, and (c) TAPPP. [Color figure can be viewed in the online issue, which is available at wileyonlinelibrary.com.]

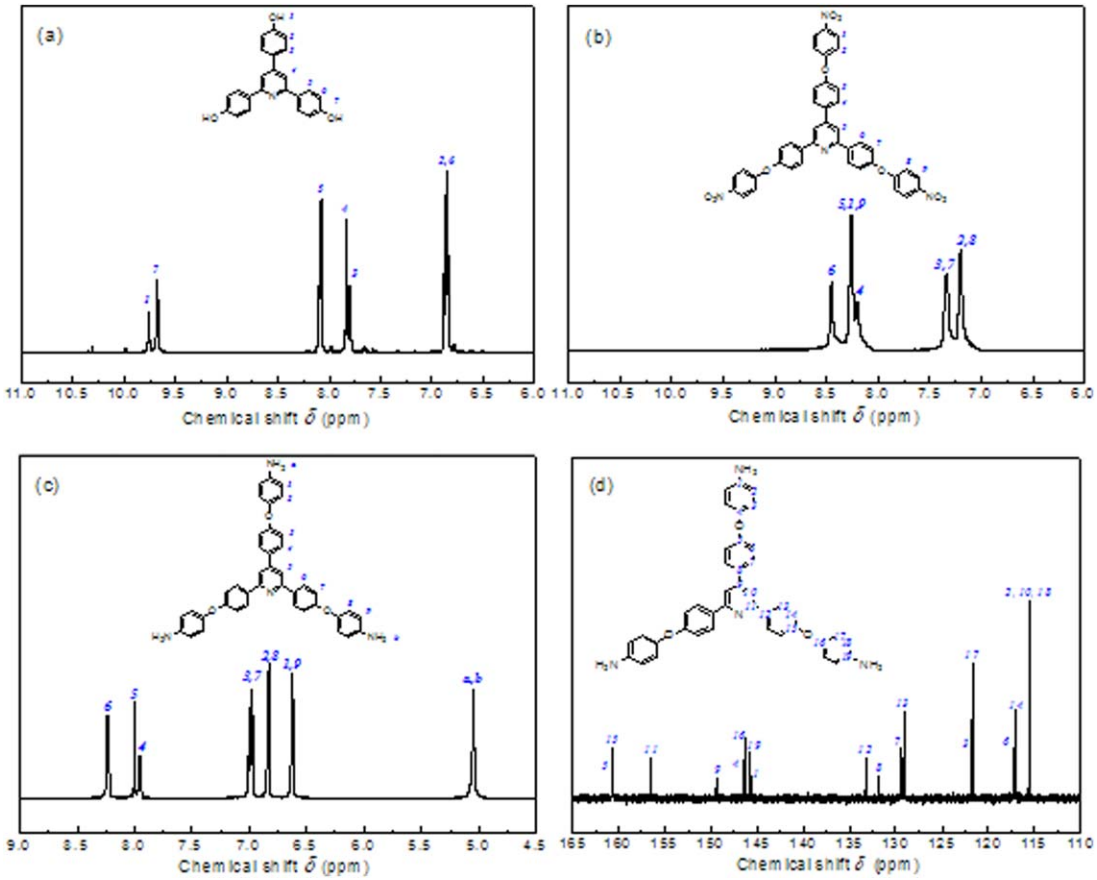

Figure 2. ^{1}H-NMR spectra of (a) THPP, (b) TNPPP, and (c) TAPPP and (d) ^{13}C-NMR spectrum of TAPPP. [Color figure can be viewed in the online issue, which is available at wileyonlinelibrary.com.]

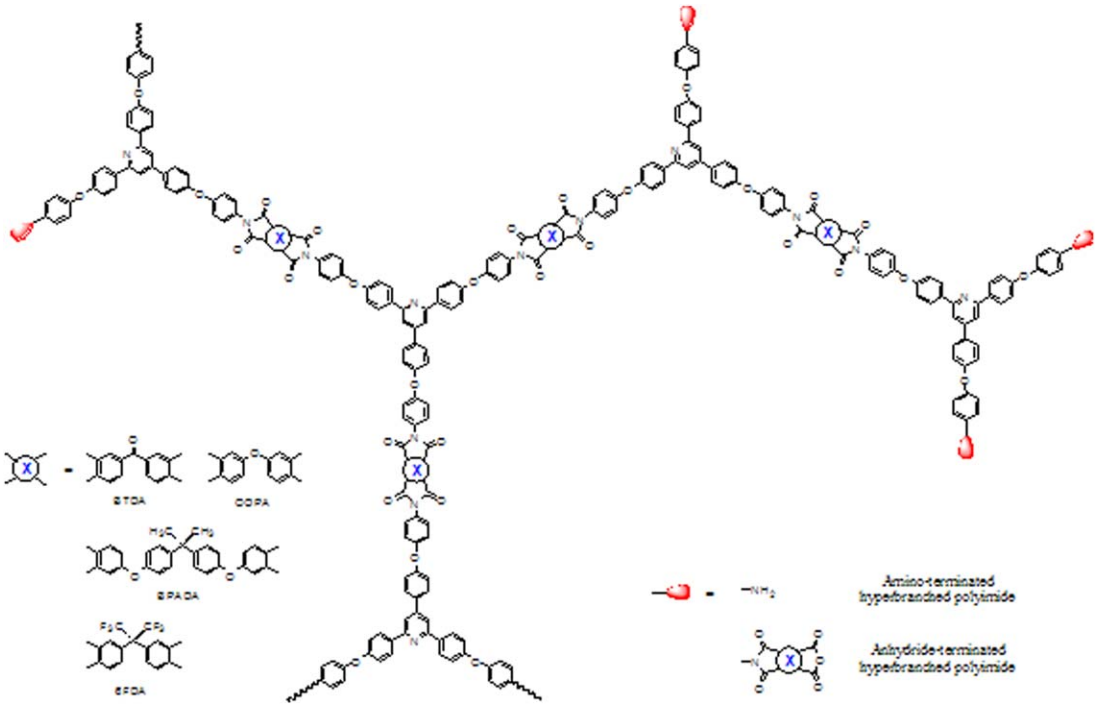

Scheme 3. Chemical structure of the novel HBPIs. [Color figure can be viewed in the online issue, which is available at wileyonlinelibrary.com.]

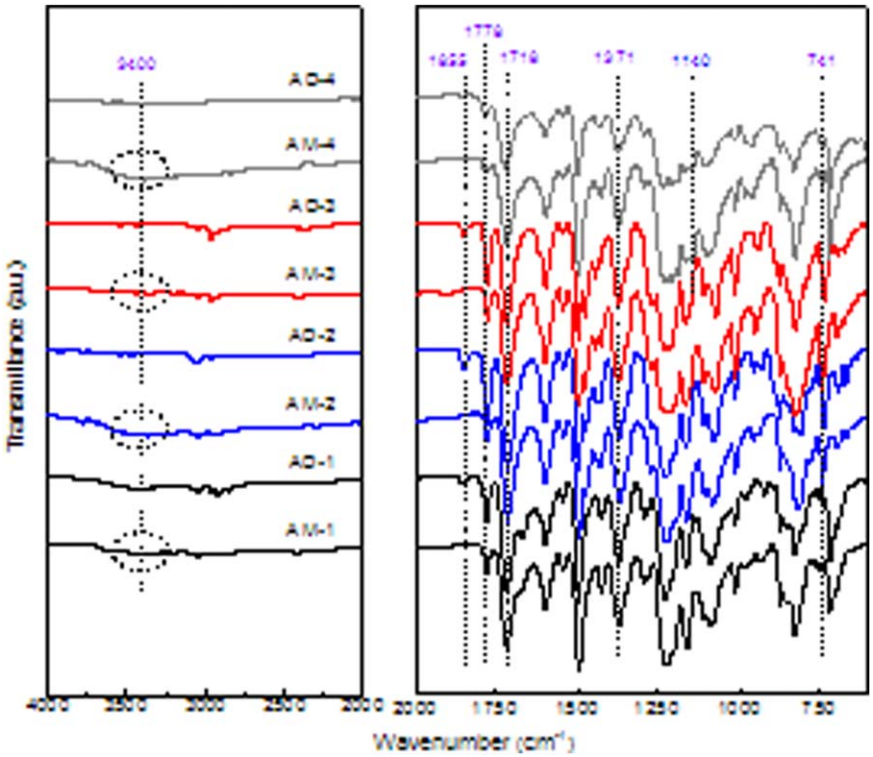

Figure 3. FTIR spectra of the resulting HBPIs. [Color figure can be viewed in the online issue, which is available at wileyonlinelibrary.com.]

synthesis of linear PIs. In the first step, hyperbranched poly (amic acid)s with different terminal groups were yielded by a different monomer addition order and molar ratios of the A_2-type dianhydride monomer and BB'_2-type triamine monomer, as previously mentioned.[39] In the second step, the AM-HBPIs were obtained by thermal imidization in the presence of *m*-xylene under refluxing; AD-HBPIs were obtained by chemical imidization with a mixture of excess acetic anhydride and triethylamine. The difference in the imidization methods was for the purpose protecting the different terminal groups.[34] The chemical structures of the novel HBPIs with different terminal groups are shown in Scheme 3.

Figure 3 showed the FTIR spectra of the resulting HBPIs. The bands at about 1778 cm^{-1} (C═O asymmetrical stretching),

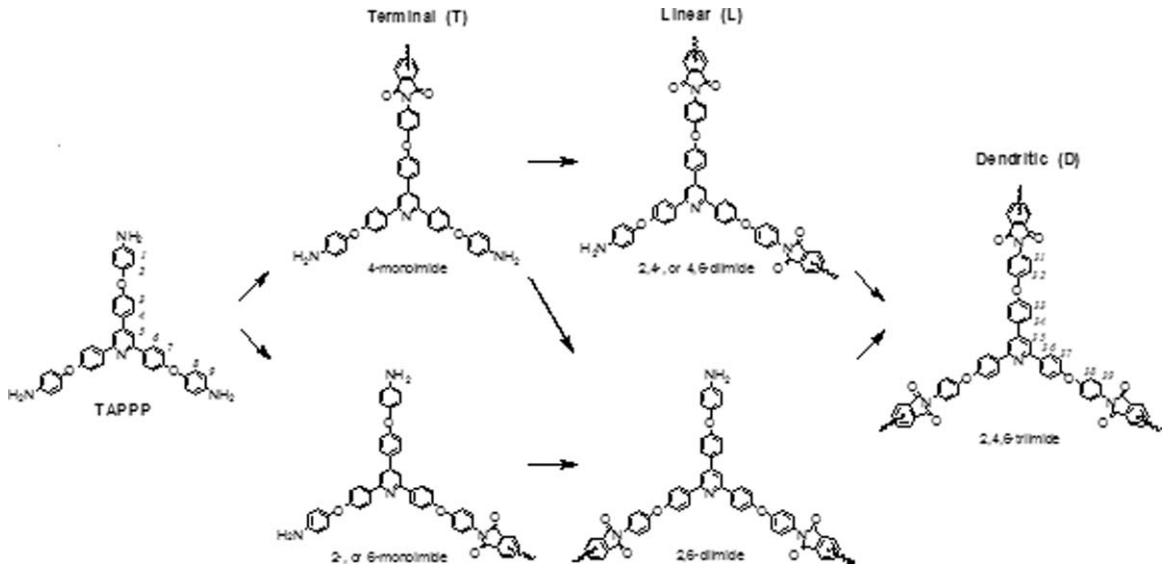

Figure 4. Possible structures of TAPPP in the novel HBPIs. [Color figure can be viewed in the online issue, which is available at wileyonlinelibrary.com.]

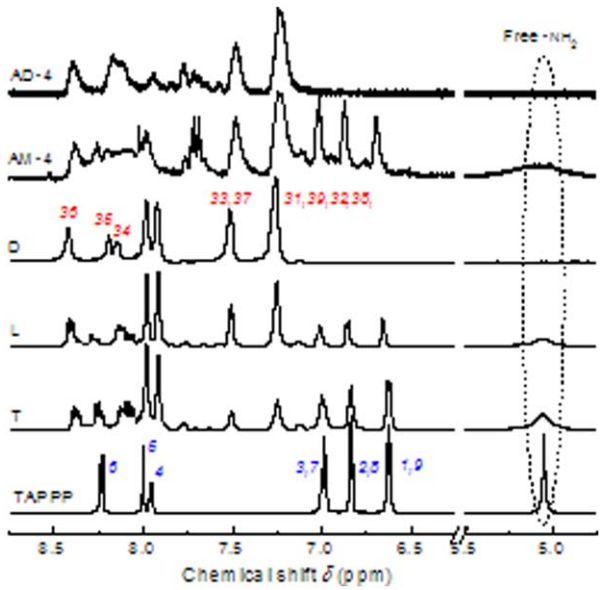

Figure 5. ^{1}H-NMR spectra of TAPPP, T, L, D, AM-4, and AD-4 in DMSO-d_6. [Color figure can be viewed in the online issue, which is available at wileyonlinelibrary.com.]

1718 cm^{-1} (C═O symmetrical stretching), 1371 cm^{-1} (C─N stretching), and 741 cm^{-1} (C═O bending) were the characteristic absorption bands of PIs. The complete imidization of the hyperbranched poly(amic acid) precursors to the target PIs was proven by the disappearance of absorption bands around 1715 cm^{-1} (C═O stretching of carboxylic acid) and 1660 cm^{-1} (C═O amide stretching). As for the AM-HBPIs, the broad absorption bands around 3400 cm^{-1} were attributed to the stretching of the N─H of terminal amine groups, whereas the bands at 1855 cm^{-1} were attributed to the stretching of the C═O of terminal anhydride groups for the AD-HBPIs. In addition, for AM-4 and AD-4, which were derived from 6FDA, we detected the characteristic absorption peaks of ─CF_3 at 1140 cm^{-1}.

All of the possible TAPPP molecular structures in the obtained polymers are illustrated in Figure 4. Terminal, linear, and dendritic units were expressed as monoimide, diimide, and triimide, respectively. The TAPPP residues in terminal, linear, and dendritic (T, L, and D, respectively) units of the HBPIs were basically same as the counterparts in analogous T, L, and D model compounds, respectively. As mentioned before,[40] the analogous model compounds of T, L, and D were synthesized by the same procedure with AM-HBPIs or AD-HBPIs but with an appropriate triamine and phthalic anhydride molar ratio. The monoimide and diimide were not easy to obtain separately because of their multiple isomers[43,44] in the actual experiment. As a result, it was hard to accurately assign the peaks in the ^{1}H-NMR or ^{13}C-NMR spectra to the protons or carbons in the terminal and linear units. We were not able to evaluate the molecular structural perfection of the hyperbranched polymers by calculating the degree of branching (DB), which was defined by Frechet et al.[45]

Table I. Yields and the [η], M_w, and PDI Values of the Resulting HBPIs

Sample	Yield (wt %)	[η] (dL/g)	M^w	PDI
AM-1	97.3	—[a]	—	—
AD-1	95.2	—	—	—
AM-2	97.1	0.45	25,000	1.92
AD-2	96.5	0.31	11,000	1.69
AM-3	97.4	0.49	32,000	2.31
AD-3	97.2	0.35	15,000	2.05
AM-4	96.2	—	—	—
AD-4	95.9	—	—	—

[a] Not measured.

Figure 5 shows the ^{1}H-NMR spectra of TAPPP; the model compounds T, L, D; and the HBPIs based on TAPPP and 6FDA (AM-4, AD-4) in DMSO-d_6. First of all, there were no proton peaks around 10.5 ppm attributed to the protons of amide bonds. This confirmed that the precursors were fully imidized for target polymers (AM-4 and AD-4). Furthermore, the peaks discontinuously distributed in the range 8.20–7.60 ppm were assigned to the protons of the 6FDA residues; this was consistent with the results by Fang et al.[46] and Chen and Yin.[47] The peaks in the range 8.45–8.05 ppm, which overlapped with the signal peaks of the protons of the 6FDA residues, corresponded to the protons in the pyridyl rings and the 2,6 position of the neighboring phenyl rings of the TAPPP residues. The peaks in the range 7.50–6.60 ppm corresponded to the protons in other phenyl rings of residues, linked both with the imide ring segments and the free amino group segments. For comparison with the model compounds T, L, and D, the broad peaks in the range 8.45–8.22 ppm were attributed to the protons in the 2,6 position of phenyl rings which were substituted in the 2,6

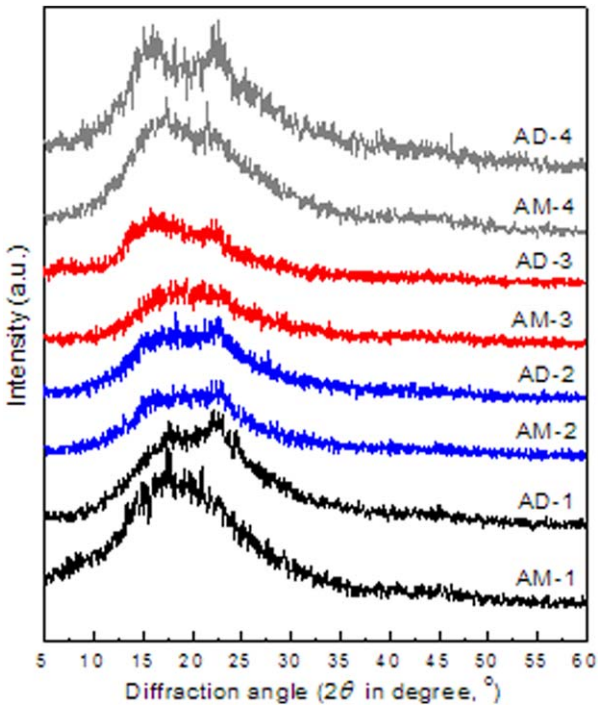

Figure 6. XRD patterns of the obtained HBPIs. [Color figure can be viewed in the online issue, which is available at wileyonlinelibrary.com.]

Table II. Solubilities of the Resulting HBPIs

Sample	*m*-Cresol	DMSO	NMP	DMAc	DMF	THF	Toluene	$CHCl_3$
AM-1	SH	PSH	SH	PSH	PSH	IS	IS	IS
AD-1	SH	PSH	SH	PSH	PSH	IS	IS	IS
AM-2	SRT	SH	SRT	SH	SH	IS	IS	IS
AD-2	SRT	SH	SRT	SH	SH	IS	IS	IS
AM-3	SRT	SRT	SRT	SRT	SH	PSH	IS	IS
AD-3	SRT	SRT	SRT	SRT	SH	PSH	IS	IS
AM-4	SH	SRT	SH	PSH	PSH	PSH	IS	IS
AD-4	SH	SRT	SRT	PSH	PSH	SH	IS	IS

SRT, soluble at room temperature; SH, soluble upon heating; PSH, partly soluble upon heating; IS, insoluble even upon heating.

position of pyridyl rings in the terminal, linear, and dendritic units. The peaks at 7.50 and 7.25 ppm corresponded to the protons in the 3,5 position of phenyl rings neighboring to pyridyl rings and the 2,6,3,5 position of phenyl rings neighboring the imide rings of the TAPPP residues, which were linked with the imide ring segments. Although the peaks at 7.00, 6.85, and 6.62 ppm corresponded to the protons in the 3,5 position of phenyl rings neighboring to the pyridyl rings and 2,6,3,5 position of phenyl rings neighboring the free amino groups of the TAPPP residues; these linked with the free amino group segments. In addition, the broad peak at 5.05 ppm was attributed to the protons of the free amine groups in the terminal and linear units. For AM-4, the DB value was impossible to determine by ^{1}H-NMR because the peaks of the T and L units were indistinguishable for their isometry, as shown in Figure 4 and 5. For AD-4, there were no peaks of the protons of free amine groups and the corresponding phenyl rings; these almost exactly matched the D unit. In other words, all of the amino groups reacted with the anhydride groups in AD-4, which should have had a completely branched structure with a DB value of 1.

Some other experimental data of the resulting HBPIs are summarized in Table I. According to the data from Table I, all of the resulting HBPIs presented high yields in the range 95.2–97.4%, and the $[\eta]$ values of the obtained HBPIs in NMP (0.8 g dL^{-1}) were between 0.31 and 0.49 dL/g. The M_w values of AM-2 and AD-2 were 25,000 and 11,000, respectively, and 32,000 and 15,000 for AM-3 and AD-3, respectively. The real molecular weights of the obtained hyperbranched polymers may have been even larger than the values measured by GPC with the linear polystyrene standard because dendritic and hyperbranched macromolecules generally have a smaller hydrodynamic size than the linear homologs with the same molecular weight and can hardly be expanded in solution.[48] The measured values of AM-2 and AM-3 were higher than AD-2 and AD-3, respectively; this was ascribed to the fact that the dianhydride monomers were more prone to hydrolyzing in the first polymerization step of anhydride-terminated polymers and the different methods of the second imidization step. Meanwhile, the lower monomer concentration of the AD-HBPIs (0.06 mol/L) compared with that of AM-HBPIs (0.08 mol/L) was another probable reason. Moreover, the measured values of AM-3 and AD-3 were a little higher than those of AM-2 and AD-2 because the hydrolysis of the dianhydride BPADA used was relative more stable than that of ODPA.[49] The PDIs of the obtained polymers varied in the range 1.69–2.31; this was attributed to the random polymerization characteristics and the monomer addition manner.[46]

Table III. Thermal Properties of the Resulting HBPIs

	T_g (°C)		$T_{5\%}$ (°C)		$T_{10\%}$ (°C)		
Sample	DSC[a]	DMTA[b]	N_2	Air	N_2	Air	R_w (%)[c]
AM-1	305.7	311.0	555.4	537.3	591.5	554.0	67.1
AD-1	256.3	264.5	550.7	520.9	573.6	551.5	61.0
AM-2	275.9	284.0	550.9	503.8	582.7	545.1	62.7
AD-2	236.4	244.8	546.6	500.0	568.7	541.7	59.5
AM-3	244.9	245.1	535.8	478.5	554.0	519.5	63.8
AD-3	218.6	224.1	529.8	465.1	553.3	506.3	59.2
AM-4	289.5	—[d]	540.1	531.9	569.3	558.0	66.4
AD-4	267.2	—	531.5	520.9	558.3	551.5	58.6

[a] T_g values obtained via DSC in N_2.
[b] T_g values obtained via DMTA with the peak temperature in tan δ curves in air.
[c] Residual weight percentages at 800°C in N_2 as obtained by TGA.
[d] Not measured.

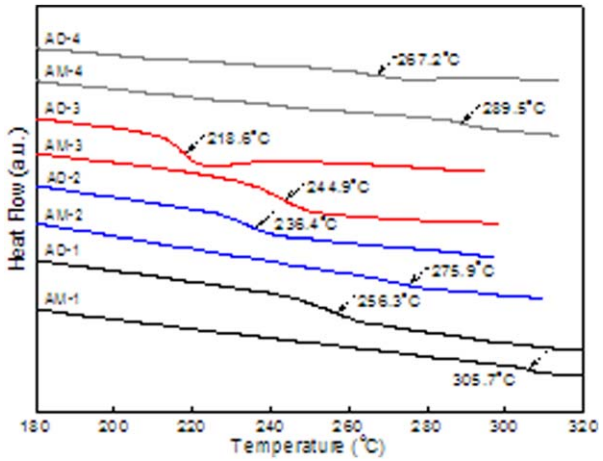

Figure 7. DSC curves of the obtained HBPIs. [Color figure can be viewed in the online issue, which is available at wileyonlinelibrary.com.]

The molecular structure, conformation and orientation were important factors in determining the properties of the polymers. The morphological information of the resulting HBPIs were obtained by the study of their XRD patterns. Generally, the degree of crystallinity of the PI depended on the imidization methods. The PI yielded by the chemical imidization method had a higher degree of crystallinity than that obtained from the thermal imidization method. This was because the former one was conducted in a solution state that might have allowed the molecular chains a more favorable conformation for stacking,[50] whereas the other one commonly induces secondary crosslinking reactions between the residual active groups in the thermal procedure. The XRD patterns of the resulting HBPI films are shown in Figure 6. Several scattered peaks in the range 15–23° in the XRD patterns were observed for AM-1, AD-1, AM-4, and AD-4, which were derived from TAPPP–BTDA and TAPPP–6FDA, respectively. This indicated that HBPIs were formed with slightly ordered structures, which were possibly induced by either the rigidity and planar structure of the anhydride segments or the high packing efficiency of polymer chains with hyperbranched structures and triphenyl pyridine units. The other HBPIs (AM-2, AD-2, AM-3 and AD-3) showed broad, ridgey diffraction patterns in the same range without clearly defined peaks; this indicated that most of the polymers were amorphous. This was ascribed to the asymmetry and irregularity of the whole polymer chains induced by the defects of the hyperbranched structure and the prolonged flexible diphenyl ether linkages; this increased the disorder and winding of the polymer chains and further resulted in a decrease in the chain-to-chain interactions and chain packing efficiency and hindered the crystallization of the polymer.

Polymer Properties

The solubilities of the resulting HBPIs were evaluated in the relevant solvents at 2 mg/mL at room temperature and at an elevated temperature for 24 h, as listed in Table II. The solubilities of the obtained HBPIs varied, depending on the dianhydride being used. The resulting HBPIs based on BTDA (AM-1 and AD-1) with rigid ketonic linkages could be dissolved only in *m*-cresol, NMP upon heating to 120°C, and partly dissolved in dimethyl sulfoxide (DMSO), DMAc, and DMF during boiling but could not be dissolved in less polar organic solvents, such as tetrahydrofuran (THF), toluene, and chloroform ($CHCl_3$), even during boiling. The limited solubility of AM-1 and AD-1 might have been due to the partially ordered structure that existed in amorphous PIs, as shown by the weak XRD peaks around 18 and 23°. The resulting HBPIs showed improved solubilities through the replacement of the rigid ketonic linkages of the dianhydride with flexible ether or isopropyl linkages. The ODPA-based HBPIs, AM-2 and AD-2, could be easily dissolved in *m*-cresol and NMP at room temperature, and in DMSO, DMAc, and DMF upon heating to 120°C, but they could not dissolved in THF, toluene, and $CHCl_3$ during boiling. The BPADA-based HBPIs, AM-3 and AD-3, could be easily dissolved in *m*-cresol, DMSO, NMP, and DMAc at room temperature and in DMF upon heating to 120°C. They could be partly dissolved in THF but could not be dissolved in toluene and $CHCl_3$ during boiling. The improved solubilities of the resulting HBPIs based on ODPA or BPADA were associated with the amorphous, broad ridgey diffraction peaks, as shown in Figure 6. The resulting HBPIs based on 6FDA (AM-4 and AD-4) with hexafluoroisopropyl linkages should have shown poor solubilities according to the XRD patterns, with several peaks scattered in the range 15–23°, but they could be dissolved in DMSO at room temperature and in *m*-cresol upon heating to 120°C and

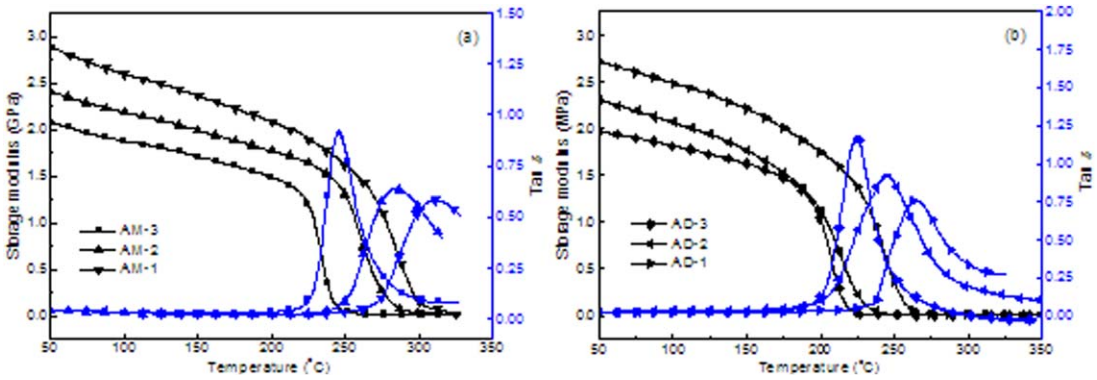

Figure 8. DMTA curves of the obtained (a) AM-HBPI films and (b) AD-HBPI films. [Color figure can be viewed in the online issue, which is available at wileyonlinelibrary.com.]

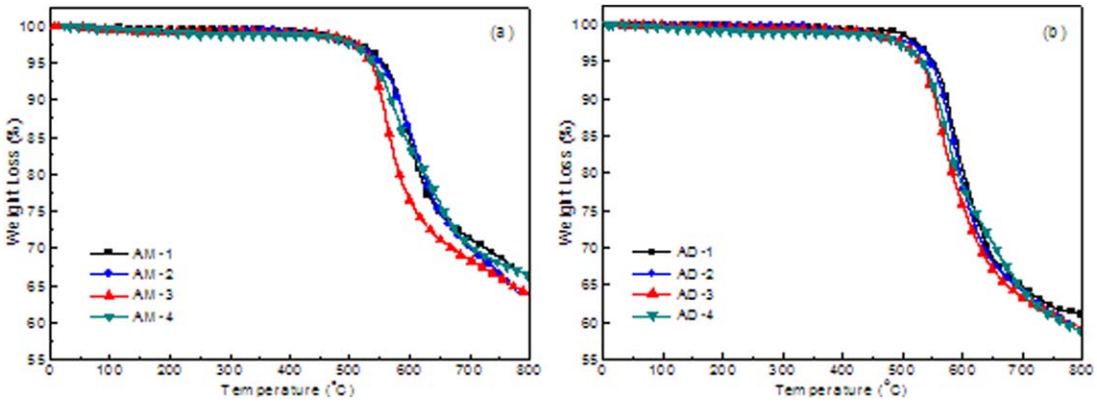

Figure 9. TGA curves of the obtained (a) AM-HBPIs and (b) AD-HBPIs in N_2. [Color figure can be viewed in the online issue, which is available at wileyonlinelibrary.com.]

partly dissolved in DMAc and DMF during boiling. These behaviors might have been due to the introduction of fluorine with a high electronegativity; this could decrease the chain-to-chain interactions of the polymers. In addition, the AD-HBPI based on 6FDA (AD-4) could be dissolved in NMP at room temperature and in THF upon heating to 50°C, whereas the AM-HBPI based on 6FDA (AM-4) could not. The differences in the solubilities between AM-4 and AD-4 might have been caused by the fluorinated terminal groups.

The thermal behaviors of the resulting HBPIs were investigated by DSC, DMTA, and TGA. The results are summarized in Table III.

The heat resistance, with indices such as the glass-transition temperature (T_g), softening temperature, and melting temperature, was the physical resistance temperature of the polymer. The T_g was taken as the ultimate-use temperature of structural polymer material in general. The T_g values of the resulting HBPIs obtained by the second heating trace of the DSC curves in Figure 7 were in the range 218.6–305.7°C, which depended on the chemical structure of aromatic dianhydride components. AM-1 and AD-1 derived from BTDA showed the highest T_g values at 305.7 and 256.3°C; this was attributed to the rigid dianhydride moieties in the polymer backbones. On the contrary, AM-3 and AD-3, derived from BPADA, showed the lowest T_g values at 244.9 and 218.6°C because of the relatively flexible polymer chains. The T_g values of AM-4 and AD-4 derived from 6FDA were between those of the HBPIs derived from BTDA (AM-1 and AD-1) and ODPA (AM-2 and AD-2). In addition, the T_g values of the AM-HBPIs were significantly higher than the T_g values of the homologous AD-HBPIs; these was attributed to the different terminal functional groups of the polymers.

In contrast, the T_g values of the resulting HBPI films obtained by the DMTA with the peak temperature in the tan δ curves, were slightly higher than those measured by DSC. The slight rises might have been due to either the different responses of the two measurements or the synthetic method of the polymer preparation. In addition, all of the obtained HBPI films showed high storage moduli (1.96–2.89 GPa) at 50°C, as shown in Figure 8. The change rules of the storage moduli of the obtained HBPIs derived from different dianhydrides or with different terminal groups were the same as those of the T_g values. As our previous work demonstrated, the T_g values of the HBPI films derived from the similar triamine without prolonged flexible diphenyl ether linkages [2,4,6-tris(4-aminophenyl)pyridine, TAPP], and those of BTDA and ODPA were in the range 311–339°C.[39] They were 20–50°C higher than those of the obtained HBPI films.

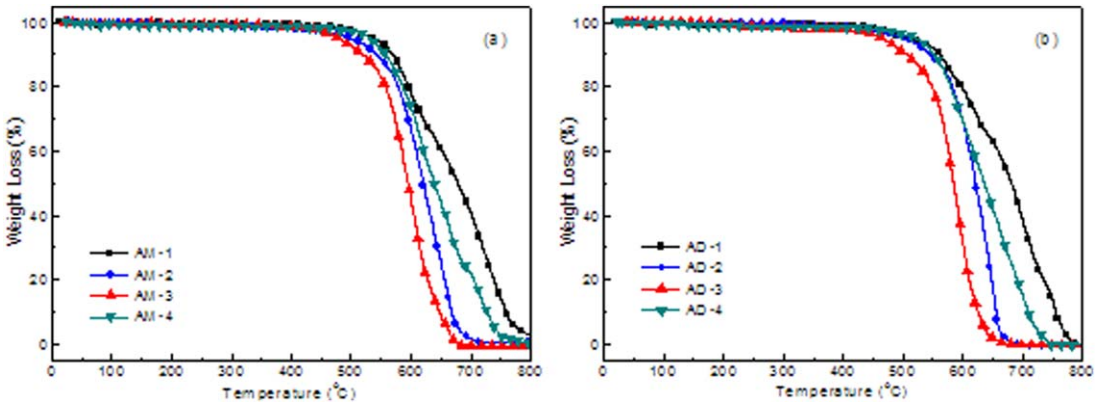

Figure 10. TGA curves of the obtained (a) AM-HBPIs and (b) AD-HBPIs in air. [Color figure can be viewed in the online issue, which is available at wileyonlinelibrary.com.]

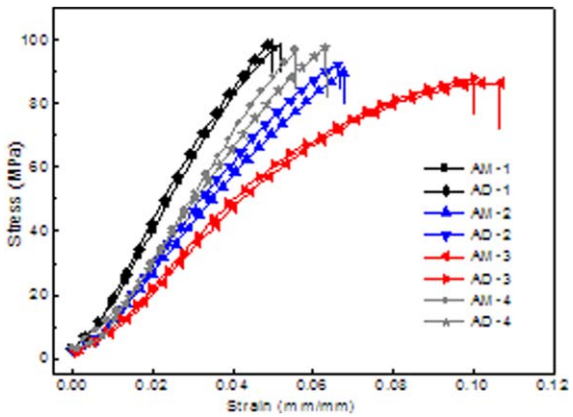

Figure 11. Stress–strain curves for the obtained HBPI films. [Color figure can be viewed in the online issue, which is available at wileyonlinelibrary.com.]

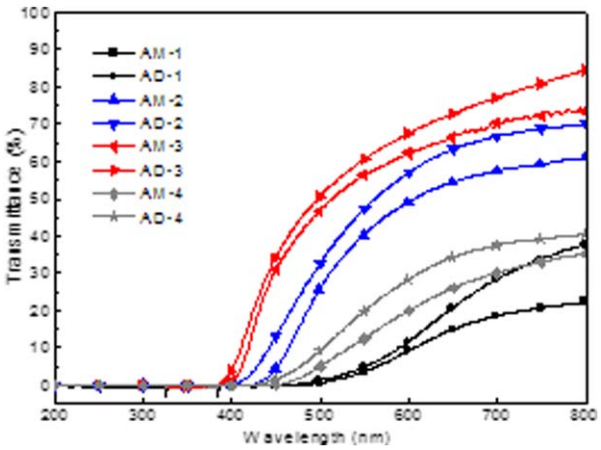

Figure 12. UV–vis transmittance spectra of the obtained HBPI films. [Color figure can be viewed in the online issue, which is available at wileyonlinelibrary.com.]

The thermal stability was the chemical tolerance of the polymer. The temperature for 5% weight loss ($T_{5\%}$) and the temperature for 10% weight loss ($T_{10\%}$) are usually considered as the criterion factors in determining the thermal stability of polymers at high temperatures. The thermal stabilities of the obtained HBPIs were evaluated by TGA both under N_2 and air atmospheres, as shown in Figures 9 and 10.

As shown in Figure 9, all of the resulting HBPIs presented good thermal stabilities without any significant weight losses up to 500°C in N_2. $T_{5\%}$ and $T_{10\%}$ values of the obtained HBPIs in N_2 were in the range 529.8–555.4 and 553.3–591.5°C, respectively. This was mainly due to the combination of aromatic segments and imide linkages with high-temperature characteristics. Furthermore, the residual weight percentage (R_w) of the obtained polymers at 800°C in N_2 were within 58.6 and 67.1%; this indicated the intrinsic fire-retardant properties of the polymers. In addition, all of the AM-HBPIs showed slightly higher $T_{5\%}$ and $T_{10\%}$ values compared with those of the corresponding AD-HBPIs; this was attributed to the different terminal functional groups. Moreover, the $T_{5\%}$ and $T_{10\%}$ values of the HBPIs derived from BTDA, ODPA, and BPADA varied from the rigidity of the dianhydride used. We found that the $T_{5\%}$ and $T_{10\%}$ values of the obtained HBPI films in N_2 were at least 30°C higher than those derived from TAPP and BTDA or ODPA.[39]

As shown in Figure 10, the TGA curves of the resulting HBPIs in air presented similar trends with those in N_2, but the corresponding temperature values were slightly lower than the former ones. The $T_{5\%}$ and $T_{10\%}$ values of the obtained HBPIs in air were reduced in the ranges 465.1–537.3 and 506.3–558.0°C, respectively. Furthermore, the weight loss of the obtained polymers in air dropped sharply to zero in the range 650–800°C. All of these might have been due to the oxidation and other correlated reactions of the polymers in the presence of oxygen under an air atmosphere. Therefore, the thermal stability under an air atmosphere is commonly known as the *thermooxidative stability.*

The introduction of a symmetrical triaryl-substituted pyridine segment, prolonged flexible diphenyl ether linkage, and hyperbranched structure into the PI backbones should be able to enhance the mechanical strength. We found that tough HBPI films were easy obtained by the casting of the corresponding hyperbranched poly(amic acid) solutions onto glass plates followed by thermal baking to remove the solvent and further thermal imidization. The stress–strain curves of the obtained HBPI films are shown in Figure 11, and the detailed data are

Table IV. Mechanical Properties of the Resulting HBPI Films

Sample	Tensile strength (MPa)	Tensile modulus (GPa)	Elongation at break (%)
AM-1	99.4 ± 3.7	2.04 ± 0.08	5.07 ± 0.46
AD-1	101.3 ± 3.1	2.01 ± 0.11	5.29 ± 0.55
AM-2	91.0 ± 2.2	1.91 ± 0.08	6.78 ± 0.41
AD-2	92.3 ± 2.6	1.89 ± 0.06	6.89 ± 0.38
AM-3	86.4 ± 1.5	1.78 ± 0.07	10.0 ± 0.35
AD-3	87.9 ± 1.8	1.73 ± 0.05	10.67 ± 0.38
AM-4	97.6 ± 3.1	1.92 ± 0.10	5.68 ± 0.42
AD-4	96.9 ± 2.5	1.94 ± 0.09	6.31 ± 0.39

Table V. Optical Properties, WA, and SCA Values of the Resulting HBPI Films

Sample	λ_0 (nm)	Transmittance at 800 nm (%)	SCA (°)	WA (%)
AM-1	474	22.4	92.1 ± 4.5	1.01 ± 0.04
AD-1	468	37.8	90.4 ± 3.7	1.15 ± 0.06
AM-2	429	61.0	89.4 ± 2.3	0.98 ± 0.03
AD-2	398	70.2	82.2 ± 4.3	1.07 ± 0.04
AM-3	382	73.4	90.2 ± 2.1	0.95 ± 0.07
AD-3	448	84.4	84.0 ± 5.4	1.04 ± 0.07
AM-4	426	35.5	97.6 ± 3.8	0.75 ± 0.02
AD-4	567	40.8	95.8 ± 3.1	0.89 ± 0.05

listed in Table IV. The average tensile strength, tensile modulus, and elongation at break varied from the dianhydrides used. The films derived from BTDA with rigid ketonic linkages (AM-1 and AD-1) showed the highest tensile strength (ca. 100.0 MPa) and tensile modulus (higher than 2.0 GPa) and the lowest elongation at break (lower than 5.3%), whereas those from BPADA with flexible ether and isopropyl linkages (AM-3 and AD-3) showed the lowest tensile strength (<88.0 MPa) and tensile modulus (<1.8 GPa) and highest elongation at break (>10.0%). The other films derived from ODPA and 6FDA (AM-2, AD-2, AM-4, and AD-4) exhibited middle mechanical indices. In comparison with the HBPI films derived from TAPP and BTDA,[39] the average tensile strength and tensile modulus values were nearly twice as high as the films of AM-1 and AD-1. The results indicate that they were strong and flexible materials, as expected.

The UV–vis transmittance spectra were measured for the thin films (ca. 0.15 mm) of the obtained HBPIs, as shown in Figure 12 and listed in Table V with the particular data. The ODPA- and BPADA-based HBPIs (AM-2, AD-2, AM-3, and AD-3) films with electron-donating linkages exhibited cutoff wavelengths (λ_0's) shorter than 430 nm and a high optical transparency with a transmittance at 800 nm in the range 61–85%, although the rest of HBPI films derived from BTDA and 6FDA with electron-drawing linkages (AM-1, AD-1, AM-4, and AD-4) exhibited λ_0 values longer than 430 nm and a low optical transparency with a transmittance of 800 nm less than 40%. Furthermore, the AD-HBPI films exhibited a higher optical transparency and shallower color than the corresponding AM-HBPI films. This might have been ascribed to the terminal auxochromic groups of the AM-HBPIs deepened the color and decreased the transparency of the films.

SCA is also an important indicator for evaluating the wettability, interfacial tension, and capillarity for waterproof, photosensor, printing, dyeing, and so on. The resulting HBPI neat films derived from BTDA, ODPA, and BPADA (AM-1, AD-1, AM-2, AD-2, AM-3, and AD-3) showed desirable average SCAs fluctuating around 90°; this indicated that the wettabilities of the obtained polymers were between the hydrophobic and hydrophilic interface. However, the resulting HBPI neat films derived from 6FDA (AM-4 and AD-4) showed average SCAs higher than 95°; this was due to the hydrophobic hexafluoroisopropyl linkages of 6FDA.

The WA of PI is an important factor for evaluating the water resistance, dielectric constant, corrosion, and permeability for electronic or microelectronic devices, gas permselective membranes, proton transfer membranes, and so on. As listed in Table V, the resulting HBPI neat films derived from BTDA, ODPA, and BPADA (AM-1, AD-1, AM-2, AD-2, AM-3, and AD-3) exhibited average WAs between 0.95 and 1.15%. This may have been due to the globular and inner empty structural characteristics of the hyperbranched polymers. Although the resulting HBPI neat films derived from 6FDA (AM-4 and AD-4) exhibited relatively low average WAs of 0.75 and 0.89% because of the hydrophobic characteristics of the fluoric linkages. Furthermore, the average WA of the AM-HBPI films was a little lower than that of the homologous AD-HBPI ones; this was attributed to the difference of the terminal groups.

CONCLUSIONS

A novel aromatic triamine, TAPPP, with a symmetrical triaryl-substituted pyridine segment and a prolonged flexible linkage was successfully synthesized and was further used as a BB'_2-type triamine monomer to prepare a series of triphenyl pyridine-containing AM-HBPIs and AD-HBPIs with several commercially available A_2-type dianhydride monomers, respectively. As expected, the obtained HBPIs with predominantly amorphous structures were found to exhibit improved organosolubilities, excellent thermal resistances and stabilities in both N_2 and air, outstanding mechanical properties, considerable optical transparency, low WAs, and neutral interface wettabilities varied from the dianhydride monomers used and the terminal groups.

ACKNOWLEDGMENTS

This work was financially supported by the Natural Science Foundation of Hubei Province (contract grant number 2013CFB007). The authors also acknowledge the Hubei Collaborative Innovation Center for Advanced Organic Chemical Materials and the Ministry of Education Key Laboratory for the Green Preparation and Application of Functional Materials for providing necessary facilities.

REFERENCES

1. Wilson, D.; Stenzenberger, H. D.; Hergenrother, P. M. Polyimides; Chapman & Hall: London, **1990**.
2. Chen, H. L.; Ho, S. H.; Wang, T. H.; Chen, K. M.; Pan, J. P.; Liang, S. M.; Hung, A. *J. Appl. Polym. Sci.* **1994**, *51*, 1647.
3. Ye, Y. S.; Huang, Y. J.; Cheng, C. C.; Chang, F. C. *Chem. Commun.* **2010**, *46*, 7554.
4. Yuan, B.; Cao, M.; Sun, H.; Wang, T.; Bu, X.; Shi, D.; Kong, Y.; Li, P. *J. Appl. Polym. Sci.* **2014**, *131*, 40338.
5. Maya, E. M.; Lozano, A. E.; Campa, J. G.; Abajo, J. *Macromol. Rapid Commun.* **2004**, *25*, 592.
6. Yan, J.; Wang, Z.; Gao, L.; Ding, M. *Polymer* **2005**, *46*, 7678.
7. Lin, C.-H.; Chang, S.-L.; Cheng, P. W. *J. Polym. Sci. Part A: Polym. Chem.* **2011**, *49*, 1331.
8. Yuan, Y.; Lin, B.-P.; Zhang, X.-Q.; Wu, L.-W.; Zhan, Y. *J. Appl. Polym. Sci.* **2008**, *110*, 1515.
9. Zhang, Q.; Li, S.; Li, W.; Zhang, S. *Polymer* **2007**, *48*, 6246.
10. Chou, C. H.; Reddy, D. S.; Shu, C. F. *J. Polym. Sci. Part A: Polym. Chem.* **2002**, *40*, 3615.
11. Zhang, Q.; Chen, G.; Zhang, S. *Polymer* **2007**, *48*, 2250.
12. Yang, C.; Hsiao, S. C.; Tsai, C. Y.; Liou, G. S. *J. Polym. Sci. Part A: Polym. Chem.* **2004**, *42*, 2416.
13. Yan, J.; Wang, Z.; Gao, L.; Ding, M. *Polymer* **2005**, *46*, 7678.
14. Zhang, M.; Wang, Z.; Gao, L.; Ding, M. *J. Polym. Sci. Part A: Polym. Chem.* **2006**, *44*, 959.
15. Liu, Y.; Xing, Y.; Zhang, Y.; Guan, S.; Zhang, H.; Wang, Y.; Wang, Y.; Jiang, Z. *J. Polym. Sci. Part A: Polym. Chem.* **2010**, *48*, 3281.

16. Hasegawa, M.; Hirano, D.; Fujii, M.; Haga, M.; Takezawa, E.; Yamaguchi, S.; Ishikawa, A.; Kagayama, T. *J. Polym. Sci. Part A: Polym. Chem.* **2013**, *51*, 575.
17. Maier, G. In The Polymeric Materials Encyclopedia; Salamone, J. C., Ed.; CRC: Boca Raton, FL, **1996**; Vol. *5*, p 59.
18. Maier, G.; Banerjee, S.; Haußmann, J.; Sezi, R. *High Perform. Polym.* **2001**, *13*, S107.
19. Monkman, A. P.; Palsson, L. O.; Higgins, R. W. T.; Wang, C.; Bryce, M. R.; Howard, J. A. K. *J. Am. Chem. Soc.* **2002**, *124*, 6049.
20. Liaw, D.-J.; Wang, K.-L.; Chang, F.-C.; Lee, K.-R.; Lai, J.-Y. *J. Polym. Sci. Part A: Polym. Chem.* **2007**, *45*, 2367.
21. Wang, K.-L.; Liou, W.-T.; Liaw, D.-J.; Chen, W.-T. *Dyes Pigments* **2008**, *78*, 93.
22. Wang, K.-L.; Liou, W.-T.; Liaw, D.-J.; Huang, S.-T. *Polymer* **2008**, *49*, 1538.
23. Wang, X.; Li, Y.; Gong, C.; Zhang, S.; Ma, T. *J. Appl. Polym. Sci.* **2007**, *104*, 212.
24. Wang, X.; Li, Y.; Gong, C.; Ma, T.; Yang, F. *J. Fluorine Chem.* **2008**, *129*, 56.
25. Zhang, S.; Li, Y.; Wang, X.; Zhao, X.; Shao, Y.; Yin, D.; Yang, S. *Polymer* **2005**, *46*, 11986.
26. Shang, Y.; Fan, L.; Yang, S.; Xie, X. *Eur. Polym. J.* **2006**, *42*, 981.
27. Yan, S.; Chen, W.; Yan, W.; Huang, M.; Chen, C.; Xu, Z.; Yeung, K. W.; Yi, C. *Des. Monomers Polym.* **2011**, *14*, 579.
28. Yan, S.; Chen, W.; Yang, X.; Chen, C.; Huang, M.; Xu, Z.; Yeung, K. W.; Yi, C. *Polym. Bull.* **2011**, *66*, 1191.
29. Huang, M.; Wang, L.; Li, X.; Yan, S.; Yeung, K. W.; Chu, P.; Xu, Z.; Yi, C. *Des. Monomers Polym.* **2012**, *15*, 389.
30. Shen, J.; Zhang, Y.; Huang, M.; Wang, W.; Xu, Z.; Yeung, K. W.; Xu, M.; Yi, C. *J. Polym. Res.* **2012**, *19*, 9857.
31. Shen, J.; Li, X.; Zhang, Y.; Wang, W.; Xu, Z.; Yeung, K. W.; Xu, M.; Yi, C. *High Perform. Polym.* **2013**, *25*, 168.
32. Flory, P. J. *J. Am. Chem. Soc.* **1952**, *74*, 2718.
33. Hao, J.; Jikei, M.; Kakimoto, M. *Macromol. Symp.* **2003**, *199*, 233.
34. Gao, C.; Yan, D. *Prog. Polym. Sci.* **2004**, *29*, 183.
35. Gao, H.; Wang, D.; Guan, S.; Jiang, W.; Jiang, Z.; Gao, W.; Zhang, D. *Macromol. Rapid Commun.* **2007**, *28*, 252.
36. Gao, H.; Wang, D.; Jiang, W.; Guan, S.; Jiang, Z. *J. Appl. Polym. Sci.* **2008**, *109*, 2341.
37. Gao, H.; Yan, C.; Guan, S.; Jiang, Z. *Polymer* **2010**, *51*, 694.
38. Itoh, T.; Gotoh, S.; Uno, T.; Kubo, M. *J. Power Sources* **2007**, *174*, 1167.
39. Chen, W.; Yan, W.; Wu, S.; Xu, Z.; Yeung, K. W.; Yi, C. *Macromol. Chem. Phys.* **2010**, *211*, 1803.
40. Shen, J.; Zhang, Y.; Chen, W.; Wang, W.; Xu, Z.; Yeung, K. W.; Yi, C. *J. Polym. Sci. Part A: Polym. Chem.* **2013**, *51*, 2425.
41. Chichibabin, A. E. *J. Russ. Phys. Chem. Soc.* **1906**, *37*, 1229.
42. Weiss, M. *J. Am. Chem. Soc.* **1952**, *74*, 200.
43. Liu, Y.; Chung, T. S. *J. Polym. Sci. Part A: Polym. Chem.* **2002**, *40*, 4563.
44. Park, S. J.; Li, K.; Jin, F. L. *Mater. Chem. Phys.* **2008**, *108*, 214.
45. Hawker, C. J.; Lee, R.; Frechet, J. M. *J. Am. Chem. Soc.* **1991**, *113*, 4583.
46. Fang, J.; Kita, H.; Okamoto, K. *Macromolecules* **2000**, *33*, 4639.
47. Chen, H.; Yin, J. *J. Polym. Sci. Part A: Polym. Chem.* **2002**, *40*, 3804.
48. Twyman, L. J.; King, A. S.; Burnett, J.; Martin, I. K. *Tetrahedron Lett.* **2004**, *45*, 433.
49. Facinelli, J. V.; Gardner, S. L.; Dong, L.; Sensenich, C. L.; Davis, R. M.; Riffle, J. S. *Macromolecules* **1996**, *29*, 7342.
50. Leu, W. T.; Hsiao, S. H. *Eur. Polym. J.* **2006**, *42*, 328.